

3D Hydrodynamic Numerical Modeling of Gorgan Bay

Seyed Mostafa Siadatmousavi^{1*}, Alireza Eftekhari²,

^{1*} Associate Professor, Iran University of Science and Technology; siadatmousavi@iust.ac.ir

² MSc Student, Iran University of Science and Technology; eftalireza@proton.me

ARTICLE INFO

Article History:

Received: 21 Jan 2023

Accepted: 15 Mar. 2024

Keywords:

Numerical Modeling
Current Speed
Temperature
Air Pressure
Rivers

ABSTRACT

Gorgan Bay (GB) is a semi-enclosed basin located southeast of the Caspian Sea (CS), Iran. The bay was registered as a biosphere reserve in 1976 and had an international focus on conservation. GB severely suffers from low water quality and water level. A hydrodynamic model was used to determine its general circulation, differences in temperature, water elevation, and current speed. This investigation includes the study of current vectors' profiles and analyzing the effects of rivers and air pressure in the circulation of this water body. The average current speed was determined to be 0.1 m/s through the bay. The lowest and highest temperatures were investigated and were -0.53°C and $+36.57^{\circ}\text{C}$, respectively. The general circulation is mostly counter-clockwise. Water elevation and temperature inside GB always follow a seasonal sinusoidal pattern. This paper neglects the effects of rivers on GB hydrodynamics due to their insignificance discharge. Also, the air pressure has a profound effect on the water level. Current vectors showed that while current speed inside this water body has decreased in the past decade, the temperature increased by almost 7°C .

1. Introduction

Gorgan Bay (GB) is a shallow water body located southeast of the CS. It is partially separated from the sea by Miankaleh Peninsula, an elongated barrier system. The bay currently has two connections to the sea through two narrow channels: Chapaghli and Ashuradeh. GB is about 60 km along the bay axis with a maximum width of about 12 km, with an average depth of about 1.8m [1].

As shown in Figure 1, the bay is relatively isolated from the sea and is characterized by significantly low wave energy [2]. The water level fluctuations of the tide in GB are negligible [3]. Therefore, tidal impacts on physical processes can be ignored, compared to the effects of wind and density gradients in GB [4,5].

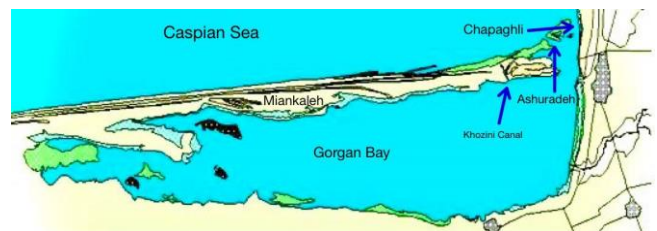


Figure 1. Gorgan Bay [26]

As one of Iran's protected environments, GB is a habitat for migratory birds and the primary habitat for sturgeon fish. GB is the only Iranian bay on the southern shores of the CS that was registered as a biosphere reserve in the Ramsar Convention in 1976. GB receives fresh water from a number of rivers and small streams that originate in the humid northern slopes of the Alborz Mountain range towards the south. This bay is mostly affected by processes within the basin. The water balance GB is affected by the infiltration of CS water, precipitation, evaporation and a smaller amount of freshwater from the river [9].

Due to the severe influence of CS on the physical properties of GB, decreasing water-level of CS has significantly increased the time residence of the water body, and also resulted in eutrophication. Based on the studies, the continuation of the warming trend of the climate governing the CS in the next century can cause the water level of the CS to decrease by 5 m in the next 75 years [6]. Sharbaty [7], while predicting the impact of the long-term process of lowering the water level of the CS on the life of GB, forecasted by the time that the water level of CS reaches -27.6 m, there is no connection to the CS. Population growth around the bay and industrial and agricultural development has also resulted in discharging wastewater into the bay, which decreased the water quality of this basin and raised some serious concerns regarding the future of this sanctuary [1].

Therefore, there is international concern about GB and the appropriate decisions to restore this water body. One of the significant prerequisites in comprehensive studies on water bodies is performing hydrodynamic research. Hydrodynamic modeling is a powerful tool for describing the flow in water basins. The hydrodynamic modeling has become a part of computational fluid dynamics with the development of technology in numerical models and advanced computing systems [8]. Among The hydrodynamic phenomena in the GB, the wind essentially has an essential role in creating the wave-driven currents, sediment transport, and morphological processes in this basin.

Other than the wind, other factors should be considered when creating the three-dimensional hydrodynamic model MIKE 3 FM Flow Model. This numerical modeling system considers the effects of bed topography, drag forces, river inflows, climatic changes in the water level, and the fluctuation of water discharge in open boundaries. Also, it can determine water levels and layered currents to successfully simulate the estuary, bay, and coastal areas. The MIKE 3 model uses the implicit method with variable direction to temporally and spatially integrate the continuity and equations of motions.

This study uses the ECMWF-ERA5 database to force the MIKE model with the required atmospheric data. To analyze the characteristics of the bay, 18 points, each in 4 layers, were examined. These points are divided into six categories. West, middle, east, mouth, boundary, and deepest part of the bay were studied. The model ran three times under three different scenarios to assess the importance of river and air pressure on the hydrodynamics of the GB as follows:

1) the comprehensive analysis of GB under real conditions.

2) The same as (1) but without the input of its main eight rivers.

3) The same as (1) but without air pressure variations.

2. Materials and Methods

The largest Bay on southern shore of the CS has an area of approximately 400 km², an average length of 60 km, and an average width of 12 km. The GB geographical coordinates are from 36.5 to 37 N and from 53.4 to 54.1 E. This Bay is separated from the CS by the Miankaleh Peninsula. Although the length of this peninsula is about 60 km and its average width is 2 km, these numbers change over time due to the Caspian Sea's sea-level rapid fluctuations [11]. The bay stretches from east to west as shown in Figure 1. A narrow and long margin of Miankaleh separates the bay from the sea. Its maximum depth is around 5 m in the southeast and its minimum depth is about 1 m in the western region. GB was connected to the sea by four canals consisting of 3 Ashuradeh islands and the Miankaleh peninsula. However, today there is only one canal between the Bandartorkman and the tip of the peninsula, the small island of Ashuradeh. The rest of the canals in the sea have dried up, the islands of Ashuradeh are connected to the Miankaleh Peninsula, and there is no more islands [12].

2.1 Hydrodynamic Modeling

Mike 3 is a 3D model developed by the Danish Hydraulic Institute (DHI). This model uses the intercellular finite volume method to discretize the governing equations of processes; such as continuity, momentum, and transfer-diffusion equations. These equations are discretized using flexible triangular cells, as shown in Figure 2. The hydrodynamic module of the model is based on the numerical solution of the Navier-Stokes equations, taking into account the Boussinesq assumptions and hydrostatic pressure for an incompressible fluid [14].

The parameters used in the hydrodynamic relations are presented in Table (1).

$$\frac{\partial u}{\partial x} + \frac{\partial v}{\partial y} + \frac{\partial w}{\partial z} = S \quad (1)$$

$$\frac{\partial u}{\partial t} + \frac{\partial u^2}{\partial x} + \frac{\partial uv}{\partial y} + \frac{\partial wu}{\partial z} \quad (2)$$

$$= fv - g \frac{\partial \eta}{\partial x} - \frac{1}{\rho} \frac{\partial P_a}{\partial x} - \frac{g}{\rho} \int_z^{\eta} \frac{\partial \rho}{\partial x} dz - \frac{1}{\rho h} \left(\frac{\partial s_{xx}}{\partial x} + \frac{\partial s_{xy}}{\partial y} \right) + F_u + \frac{\partial}{\partial z} \left(v_t \frac{\partial u}{\partial z} \right) + u_s S$$

$$\frac{\partial v}{\partial t} + \frac{\partial v^2}{\partial x} + \frac{\partial uv}{\partial y} + \frac{\partial vw}{\partial z} \quad (3)$$

$$= fu - g \frac{\partial \eta}{\partial y} - \frac{1}{\rho} \frac{\partial P_a}{\partial y} - \frac{g}{\rho} \int_z^{\eta} \frac{\partial \rho}{\partial y} dz - \frac{1}{\rho h} \left(\frac{\partial s_{yx}}{\partial x} + \frac{\partial s_{yy}}{\partial y} \right) + F_u + \frac{\partial}{\partial z} \left(v_t \frac{\partial v}{\partial z} \right) + v_s S$$

2.2 Model Setup

This study uses the Iranian National Institute for Oceanography field data of 5 RCM instruments to calibrate the model. The ECMWF-ERA5 database was used to implement the MIKE model with data along with important river inputs, bed resistance, atmospheric radiation data, and sea level air pressure changes. The bathymetry map is one of the most critical inputs of hydrodynamic models because there needs to be more precision in modeling the geometric boundaries to simulate the desired phenomenon correctly. The Iranian National Institute provided the bathymetric data for simulations.

Table 1. Parameters used to present model equations

Parameter symbol	Parameter definition	Parameter symbol	Parameter definition
$h = \eta + d$	Total water depth	Z,y,x	Cartesian coordinates
w,v,u	Flow velocities in order z,y,x	η	Water level elevation
$f = 2\Omega\sin\phi$	Coriolis force	D	Constant water depth
ρ	Water density	G	Earth's gravitational acceleration
$S_{xx}, S_{xy}, S_{yx}, S_{yy}$	Reflective stress tensors	V_t	Vertical vortex viscosity
P_a	Atmospheric pressure	ρ_0	Water reference density
u_s, v_s	The velocity of water flowing from a point source	S	Discharge Springs

The measurement file was completed in the Mesh Generator-MIKE ZERO environment. The selection of the computing network should be done according to the accuracy and cost of computing so that the results are independent of the computing network. A grid with a large size causes wrong results, and a grid with a minimal size causes the volume of calculations to increase tremendously. After making a series of volumetric files and testing the accuracy of their results, the file presented in Figure 2 was selected as the optimal computing grid [8].

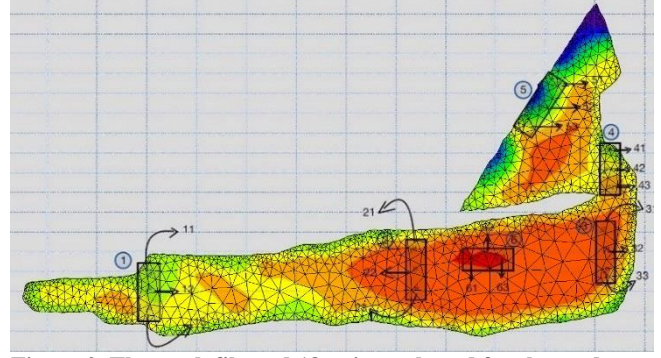


Figure 2. The mesh file and 18 points selected for the study

Wind force has been used as a variable in space and time as an essential factor in shaping the currents of the Bay and gathered from the ECMWF data center to investigate the current patterns of GB. In addition, the inflow discharge of 8 rivers to GB (Qarasu, Baghu, Gaz, Sar Kalaneh, Nokandeh, Golugah, Rostam Kala, and Behshahr) has been incorporated. The boundary conditions of water level fluctuations were enforced to the boundary using outputs of a large-scale calibrated FVCOM model [10].

To include the effects of solar radiation, the data of air temperature, relative humidity, and 2m surface temperature of GB from the data of the ECMWF-ER5 database, which have sufficient accuracy in performing numerical modeling, have been used. Latent heat, sensible heat, short and long wave radiation are all numerically entered into the model according to Valizadeh [10].

A four-layered 30 seconds time steps Mike 3 FM model was performed to simulate a three-dimensional pattern due to wind, bottom topography, precipitation, evaporation, air pressure, and principal rivers leading to GB. Three years of the simulation were performed to investigate such effects on the hydrodynamics of GB. Four sigma layers were employed as more layers only increased the cost of calculations and did not have a significant effect on the accuracy of the results. Barotropic pressure modeling and vortex viscosity are considered with the Smagorinsky formulations with a constant value of 0.28. Also, bed resistance roughness was set at 0.05 m.

2.3 Calibration, Validation, and Stability

The calibration process was performed by comparing the Iranian Institute for Oceanography field measurements of the measured points with the model output. In Table (2) and Figure (3), the names and locations of five measuring stations by the National Institute of Oceanography are evident. From August 10, 2019, to August 25, 2019, the temperature and current speed at these points were measured and recorded by the National Institute of Oceanography. Pearson's correlation coefficient was used to study model output and field data accuracy. For a statistical population, the correlation coefficient of the population is defined as follows:

$$\rho_{(X,Y)} = x = \frac{\text{cov}(X,Y)}{\sigma_X \sigma_Y} = \frac{E[(X - \mu_X)(Y - \mu_Y)]}{\sigma_X \sigma_Y} \quad (4)$$



Figure 3. Locations of RCMs

Table 2. Stations, position, and depth of RCMs

Installation Depth (m)	Installation Position		Stations
	Longitude	Latitude	
1.1	54° 2.355'E	36° 53.919'N	RCM9-1
1.5	54° 2.212'E	36° 53.952'N	RCM9-2
1.8	54° 1.918'E	36° 54.022'N	RCM9-3
2.4	54° 1.536'E	36° 54.113'N	RCM9-4
2.5	54° 1.322'E	36° 54.163'N	RCM9-5

where *cov* is the covariance, σ_X is the standard deviation of variable *X*, μ_X is the mean of variable *X*, and *E* is the mathematical expectation. According to this method, model output and field data's correlation coefficient is 0.72. Figure (4) shows the temperature measured in the middle of the mouth at a depth of 1.8 m by the device installed at this depth in a period of 2 weeks compared with the modeling data.

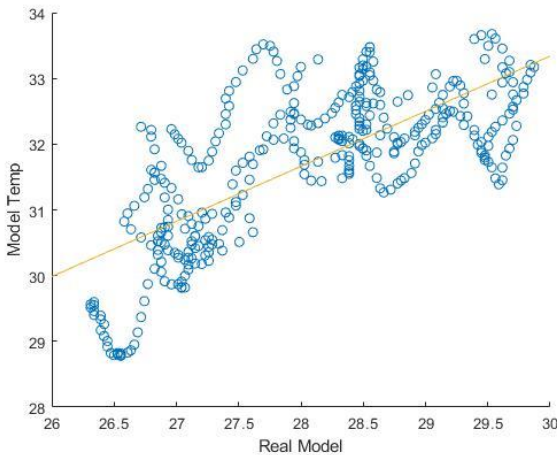


Figure 4. Calibration of Model and in situ data

3. Results and Discussion

As shown in Figure 2, 18 points, each in 4 layers, were examined to analyze the Bay's temperature. These points are divided into six categories. 1. West, 2. Middle, 3. East, 4. Mouth, 5. Boundary, and 6. The deepest part of the Bay was studied. Each of these sections was studied separately and compared with each other. For better identification, these points are

coded so that the first digit from the left represents the studied profile, and the next two digits are the location of the discussed point and the layer where the point is studied, respectively.

As shown in Figure 5, the temperature fluctuations were studied across the entire Bay. The temperature inside the Bay has changed sinusoidal in all places and all layers during different seasons. The study of temperature changes revealed that the lowest temperature reaches -0.05°C , and at the highest temperature, it reaches $+36.5^{\circ}\text{C}$. It should be noted that with all existing similarities, the average temperature of the entire Bay is 20.4°C , and also, due to the heat received from the sun, the average temperature in the surface layer experiences a higher temperature than the average temperature in the bottom layer of GB.

Another issue that should be mentioned is the visible temperature difference at different points on the surface and bottom of GB in the same period. In the winter season, we experience a temperature difference of more than 12°C on the surface of the western part of the bay and the model border. This temperature difference can also be seen with a slight decrease at the entrance of the bay, so that in the hot season, on average the surface and bottom of the GB in the western part experience a lower temperature than the eastern areas. This temperature difference, although insignificant, can also be seen from the north to the south of the Bay; so, as we move from the northern coasts (Miankaleh) to the southern coasts, we will see an increase in temperature.

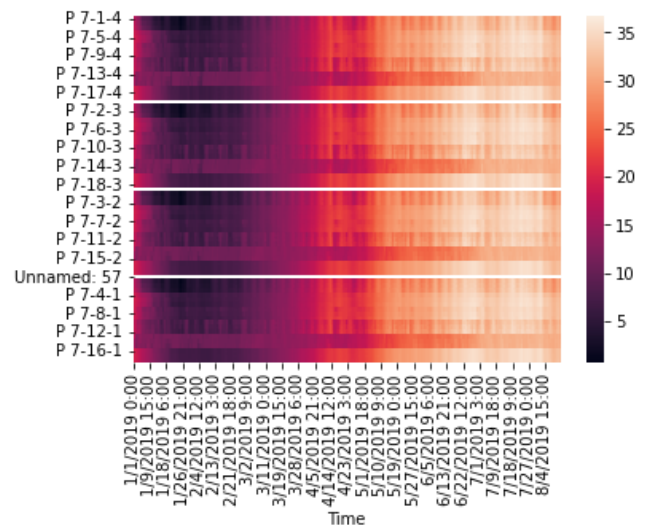


Figure 5. Temperature at different points inside GB

3.1.1 Western section of the Bay

In the western part of the bay, which is more affected by changes in temperature and water level of GB due to its distance from the mouth of the bay, its depth, and also due to the topography of the region, the temperature has similar behavior in all layers. The research results indicate that the water temperature in

GB is greatly influenced by the seasonal temperature fluctuations of the bay.

The temperature on the northern coast of the western side of GB experiences a temperature difference of 1°C on average in all seasons of the year. The average temperature is relatively high from 11 June to 9 September in all layers, and the temperature of 35.6°C is the highest temperature calculated in the layer near the bottom of the bay. The lowest temperature was measured as -0.53°C in the surface layer on the northern shores of the western part of GB. In all layers, as we move from the northern coasts to the southern coasts, it gets hotter, as well as the middle of the bay in the western part, which experiences its lowest temperature in the bottom layer of the bay. Also, the temperature gradually decreases from the surface to the bottom of the Bay.

3.1.2 Middle section of the Bay

The temperature changes in the layers are noticeable in the middle part of the Bay since the most significant depth of the Bay is located there. GB receives fresh water from several rivers and small streams that originate in the humid northern slopes of the Alborz Mountain range towards the south [18]. In the summer season, we see the highest temperature on the southern coasts, and in the winter season, we see the lowest temperature. Most temperature fluctuations occur on the southern coasts of GB. Unlike the western part of the bay, in the deep part of the bay (middle), the distance between the temperatures in different layers is more different as the depth increases. In the middle part, the temperature changes fluctuated between 2.56 and 36.62°C; Thus, GB is very much affected by seasonal temperature fluctuations in the Bay. Like the western part of the Bay, the maximum and minimum temperatures occur in July and January, respectively. The average temperature in this profile is 20.7°C, and it should be kept in mind that as the winter season approaches, the temperature will decrease as one moves from the northern coast to the southern coast. This process of change will be repeated in all layers.

3.1.3 Eastern section of the Bay

The eastern part of GB is the closest point to the mouth of the Bay and the rivers that flow into it. Various permanent and seasonal rivers flow into the Bay from the southern and eastern parts of the Alborz Mountain range, including the Qarasu and Gorganrod rivers in the northeast of the Bay, with an average discharge and annual sediment of about 0.5 million cubic meters and 3.5 million tons are the most important of them. GB, in January and March seasons, experiences relatively lower temperatures in all layers compared to the western and central part of the Bay, but the behavior of those places, like other parts of the

interior of the Bay, is seasonally fluctuating. Its maximum and minimum, like in other places, happened in July and December.

Another noteworthy point in the eastern part of the Bay is its temperature behavior. The eastern areas near the mouth of the Bay feel lower temperatures in summer than the middle-eastern and the southeast part of the Bay. Also, they are the warmest point among profiles 1 and 2 in the winter season. By moving from the northeast to the southeast, the minimum temperature decreases. With a temperature of 2.4°C, the minimum temperature in the surface layer southeast of the Bay occurs in profile 3.

3.1.4 Mouth of the Bay

Temperature changes in the winter season are not more significant in any place inside GB than outside its mouth. Ashuradeh mouth - Bandar Turkman, located in the northeast of GB (approximately 400 m wide, 3 km long, 1.5 m average depth), where intense water exchange with GB takes place, witnesses a minimum temperature range of 2.56 and a maximum of 35.96°C. In winter, there is a temperature difference of more than 8°C in just over two days.

In the research conducted in the past by Ranjbar and Hajizadeh [3], they also witnessed seasonal temperature fluctuations in the GB and reported the maximum and minimum temperatures in the seasons of July and December. The temperature range of the bay in this research was at a minimum temperature similar to the current research, but the highest temperature recorded in their research was 29.2°C, which is lower than the current study, which may be due to the difference in the years in which the modeling was done. This finding indicates the warming of the bay over time, which is considered a climate risk and may eventually lead to the destruction of the bay.

3.1.5 Boundary of the Model

The highest minimum among all points in GB was recorded at model's boundary. The lowest temperature is 7.7°C, and the highest temperature is 32.4°C, which is the lowest among other parts of the Bay. In the bottom layer of GB, we see a temperature range of 9.91 to 31.83°C at point 511 near the model boundary. The border points of the model have the lowest temperature in the summer season and the highest temperature in the winter season.

3.1.6 The comparison of temperature of the Mouth and the Farthest Part from the Mouth

Six points have been identified in the mouth of GB and the western areas of GB, which are further away from the mouth. The minimum temperature of the mouth of the Bay is 2°C warmer than the temperature of the western parts of GB. The study shows that the mouth and the west of the Bay experience the exact temperature of 35°C in summer. However, these two

points will feel a temperature difference of nearly 10°C in winter. The mouth of the Bay experiences a much higher temperature. The temperature difference in the mouth of the Bay and the western areas reaches its maximum value from 10 December to 10 March. This difference of nearly 10°C is continuously repeated in all layers. It is worth noting that in most of the modeling time, the mouth of GB feels a higher temperature than the western region of the Bay.

3.2 Water Level

The pattern of water level changes in GB, which is shown in Fig (6), is similar in the western, central, eastern, and deep parts, with few differences, and most fluctuations in the water level occur at the mouth of the bay and the boundary of the model in the CS. It is known that water level fluctuations in GB have a seasonal behavior such that from April to mid-August, the trend of surface water fluctuations in the Bay increases, and from mid-August to mid-February, a decreasing trend occurs, but with high fluctuations.

Fluctuations of the water level in the western part with an average, a minimum, and a maximum of 0.02, 0.04, and 0.22 m, respectively. From the western part of the Bay to the middle, there is an increase in depth and the height of surface fluctuations; So, in the middle part of the Bay, average and minimum fluctuations are 0.03 and 0.22 m, respectively. Fluctuations in the eastern part of the Bay behave similarly to the western part and maintain their average of 0.02 m. There is a sinusoidal behavior in the water height at the boundary of the model so that in the second six months of the year, it has a downward behavior, and in the first six months of the year, it has an upward behavior. It is worth mentioning that the deepest area of GB shows a maximum height fluctuation of 1.19 m.

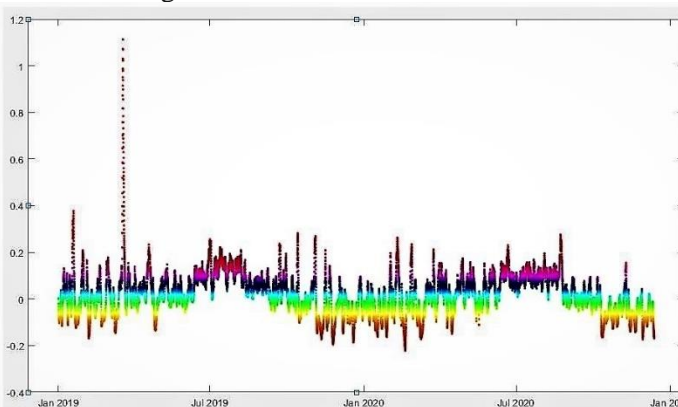


Figure 6. Time series of water level of GB

3.3 Current Speed

As shown in Figure 2, the speed of surface currents was studied at 18 points across GB in four layers. The speed of the currents is shown in Fig (7). At the mouth and the boundary of the model, currents were more substantial than others. Based on the modeling results,

the surface layer of water and the bottom layer of GB have a noticeable difference in the speed of currents.

3.3.1 Western Part

The current speed near the southern shores of the Bay in the surface layer is lower than that of the northern shores. From north to south in the western part of the Bay, there was a downward trend in the speed of currents, and the average speed in the northern and southern parts was 0.03 and 0.02 m/s, respectively.

In the layer near the bottom of the GB, the speed of currents in all western parts is more uniform, and they experience lesser fluctuations, unlike the surface layer of the Bay. The average speed in this part is 0.015 m/s, and the maximum speed is 0.01 m/s, slightly higher in the southern part than in the northern part.

3.3.2 Middle Part

The speed on the northern coast in the central part is higher than on the southern coast of this part. The maximum speed is 0.16 m/s in the northern part and 0.1 m/s in the southern coasts, and the average speed of the differential currents is 0.06 m/s. A noticeable difference can be seen between the layer near the sea floor and the surface layer. The speed in the surface layer is higher on the southern coasts than on the northern coasts, but the highest speed occurs in the center of this section. It is worth mentioning that from the bottom of the north to the south of this section, the speed is 0.02 m/s.

3.3.3 Eastern Part

In this section, the difference in the speed of currents in the northern and southern parts was 0.02 m/s. The average speed close to the mouth of the Bay, the central part, and the southern part are 0.34 m/s, 0.19 m/s, and 0.11 m/s, respectively. Like point 314, this layer has the highest speed; after that, the center and south of the Bay experience faster speed respectively. This section's maximum speed currents is 0.23 m/s in the northern part.

3.3.4 Mouth of the Bay

The speed increases from the north of this area to the south. At point 414, the average speed was 0.74 m/s, and the maximum speed was 0.79 m/s. Meanwhile, at point 434, the average and maximum speed, the highest value in the whole bay, are 0.12 and 1.1 m/s, respectively. In the bottom layer, in each region, speed decreases, but the increasing trend of flow speed remains the same from 414 to 434. So the average at point 414 is equal to 0.051 m/s and at point 434 is equal to 0.088 m/s.

3.3.5 Boundary of the Model

In the surface layer at the model's boundary, we see homogeneous velocity fluctuations, the maximum of which is 0.44 in the center of this section, and the average is 0.09 m/s. In the bottom layer, the flow velocity fluctuations have the same trend as the surface layer; the only difference is that they have a difference of 0.1 m/s with the surface layer at all points.

3.3.6 Deepest part of GB

The bay's mid-bottom was studied in this section, which is the deepest part. Its center's maximum and average speeds are 0.1 and 0.017 m/s, respectively.

3.4 Study of flow vectors

This study has been done in twelve seasons, the results of the first three have been ignored so that the model is stable and the results are reliable.

3.4.1 Spring

In April, the intensity of currents at the mouth of the bay is very high, and in fact, the highest intensity of currents in GB has been witnessed in this place. Also, currents from west to east can be seen on the northern and southern coasts, considering that the density and intensity of these currents are more visible on the northern coasts than on the southern ones. An eddy current is formed in the center of the bay and the shallow part.

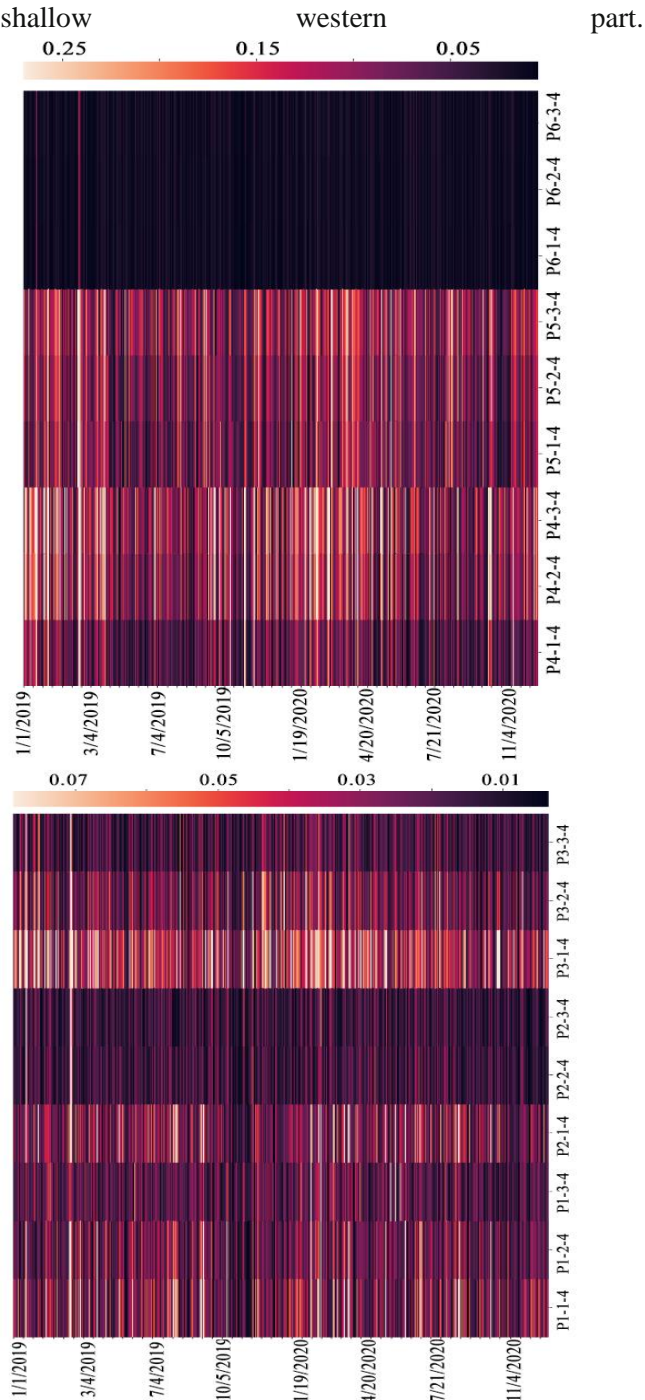


Figure 7 Surface currents of GB – Surface layer of every profiles from north to south coasts

Notably, the model results show the difference in the water level inside and outside GB. The model shows a difference of three centimeters inside the bay compared to its outside. From mid-May to mid-June, we see an increase in the water level in the bay. This increase in level leads to a difference in the level inside the bay so that the right side of the bay is more than one centimeter higher than the western part. The water level continues to rise until the end of the season, but this water level difference can still be seen inside the bay.

The current vectors show that the density and intensity of the current are higher on the northern coasts than on the southern coasts. It also indicates a current from the entrance into GB, and eddy currents are seen in the middle and west of it.

3.4.2 Summer

In the surface layer of the bay, there is a trend from west to east. In this layer, the north shores experience more current than the south shores, and a vortex forms near the mouth of the bay. In this layer, during the summer, the intensity of currents in the shallow part is less and remains constant in the deep part. In the deep part of the bay, there is a counter-clockwise eddy all summer long. The intensity of the currents in the bottom layer, on the north and south coasts, decreases during the summer.

The trend of increasing the water level inside GB continues in July and reaches the most considerable difference in the water level inside the bay in the summer season. During the whole summer, the difference in the level of the eastern and western parts inside GB is quite evident. In July, the currents on the northern coasts are more than on the southern coasts, the density of currents is witnessed at the mouth of the bay, and the eddy currents are visible in the central and western parts of the bay.

In August, the speed of the currents in the north and south coasts and the mouth of the bay reach their lowest level. However, still, the difference in the balance in the eastern and western parts of the bay is seen. From mid-September to mid-October, there is a decrease in the GB's water level, and the currents in the north and south coasts and the mouth of the bay experience a significant increase compared to last month.

3.4.3 Autumn

The currents become more robust and denser as we move toward the mouth of the bay. The currents on the north and south coasts are from west to east. In addition, to counterclockwise eddies, currents from west to east can be seen in the middle of the bay. As November and December are approaching, this time, it is the west of the Bay that has a higher average level than the east. The currents have lost their speed,

density, and intensity in the coasts and mouth of the bay.

3.4.4 Winter

In the winter season, we see a change in the average water level so that in January, the western part of the bay has a higher level than the eastern part. However, this trend changed in March, and this is the right part of the bay, which has a higher average level than the western part. Regarding the currents, as the end of winter approaches, the speed of the currents in all parts is increasing.

3.5 Profiles of flow vectors

This study has been done in four seasons; the results of the first three months of the model have been ignored so that the model is stable and the results are reliable.

3.5.1 Spring

Currents in April in the surface layer and the bottom layer follow a similar trend most of the time. In the surface layer, the flow vectors move toward the opening. The flow density at the opening and boundary of the model is very high. In the bottom layer, the speed of currents in the deep part of the bay is negligible. In May, most of the currents in the surface layer were towards the inside of the bay; the intensity of the currents in this layer near the north and south coasts was higher than the bottom layer.

In the surface layer, a series of currents move from the southern coast to the northern coast, and we also see counterclockwise eddy currents in the deep part of the bay. In June, in the surface layer in the deep part of the bay, currents are from east to west, but on the northern and southern coasts, these currents are along the coasts from west to east. In the bottom layer, counterclockwise eddies occur in the deep part of the bay.

3.5.2 Summer

In the surface layer of the bay, there is a trend from west to east. In this layer, the north shores experience more current than the south shores, and a vortex form near the mouth of the bay. In this layer, during the summer, the intensity of currents in the shallow part is less and remains constant in the deep part. In the deep part of the bay, there is a counter-clockwise eddy all summer long. The intensity of the currents in the bottom layer, on the north and south coasts, decreases during the summer.

3.5.3 Autumn

In the surface layer, counterclockwise eddy currents are formed in the deep part of the bay in October. The currents in the crater are strong, and over time, their intensity decreases during the fall. Currents on the north and south coasts are from west to east. In this layer, in November, the main currents are from west to east, and of course, these currents are insignificant, such as the currents near the north and south coasts. In

December and early January, currents move from the mouth into the bay, and a vortex can be seen in the shallow part of the bay, which is located in the west of the bay, during autumn. In the bottom layer, the current on the southern coast is negligible. In this layer, the deep part of the bay has a small current towards the mouth of the bay during autumn, except in November, when eddy currents are seen in the deep part of the bay again.

3.5.4 Winter

In the winter season, two currents occur in two different directions in the surface layer and bottom of GB. The flow in the surface layer is from the mouth to the inside of the bay during winter. Since the middle of January, there have been currents on the northern coasts, but they are not seen on the southern coasts. These currents are insignificant in the deep part of the bay. Moving towards February, the currents become much more potent and can be seen in the mouth, north, and south coasts, as well as in the deep part of the bay. Just like the surface layer of the bottom layer, a similar trend is created for currents during winter; currents move from the bay's sides to the outside.

3.6 Effects of main rivers

GB receives fresh water from several rivers and small streams that originate in the northern wet slopes of the Alborz Mountain range to the south. The construction of dams and the use of freshwater resources in agriculture worsens the bay's condition because of the decrease in the water output of the Gorgan River, Qarasu, and other rivers, as well as the drainages leading to the southern part of the bay. In the last two decades, the rapid drop of the sea level by 150 cm has created unexpected water exchange conditions between the sea and the bay by the existing waterways.

It is evident that the level inside the bay has no significant relationship with the rivers and only depends on its topography and the currents entering its mouth. A model run without considering rivers showed that currents in winter and summer near the northern and southern shores of the Bay cause slight changes in the water circulation pattern. Regarding the velocity vectors, it should be mentioned that only in the layer close to the bottom of GB did minor changes occur on the northern coasts from mid-December to mid-January. These changes can be seen on the southern coasts from mid-August to mid-September.

3.7 Effects of air pressure

In the equations of motion, pressure changes can cause flow changes and create flows on a large scale. It is gathered that the water level inside GB depends on the pressure parameter and the differences are evident in almost all year seasons. Also, velocity vectors affect the pressure parameter near the northern and southern coasts of the Bay from mid-May to mid-June. The lack of pressure has affected the average velocity of currents; So, in the winter season, the

intensity of the velocity vectors in the surface and bottom layer of the bay is less than in no-pressure state. In addition, the absence of pressure in May and June in the bottom layer of the areas near the coast has

eastward. In deeper areas, there was westward transportation. Therefore, the circulation of water in GB was composed of gyres. These findings were in agreement with the findings of previous studies [8,

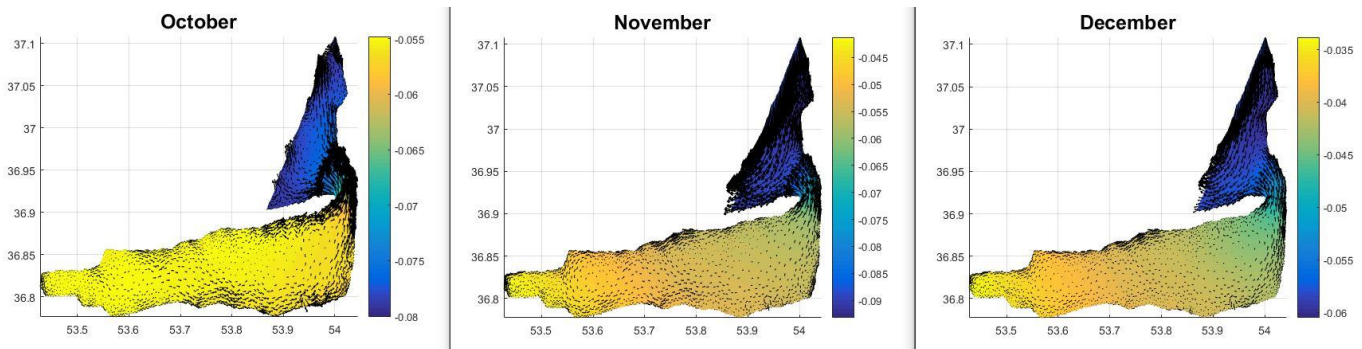


Figure 8. Currents vectors and Water Level in Autumn

reduced the intensity of the current vectors.

4. Conclusions

A bay is a geomorphic and sedimentary basin with a distribution controlled by the geological setting, climate, hydrology of the rivers, eustatic conditions, and the hydrodynamics of waves and longshore currents [19]. Transitional waters such as bays are often exposed to a wide range of stresses associated with the dense human population inhabited by coastal regions. [20] [21] In this research, GB, one of the thirteen biospheres inside the borders of Iran, was studied. This bay was registered as a biosphere reserve in 1976, and there is an international view on its protection [22].

This research studied the fluctuation of hydrodynamic objectives, such as water surface elevation and current speed, under three scenarios to provide findings that can make available important information on adapting suitable decisions relating to the management and restoration of water bodies. The water circulation inside this basin is counterclockwise and a function of wind-induced currents in all the layers. In shallower areas, the transportation of water masses was eastward. In deeper areas, there was westward transportation. Therefore, the circulation of water in GB was composed of gyres. These findings were in agreement with previous studies' findings [3].

The average current speed inside the bay is 0.1 m/s, which is lower than previous studies conducted because water exchange between GB and the Caspian Sea has reached an all-time low. The water circulation inside this basin is counterclockwise and a function of wind-induced currents in all the layers. In shallower areas, the transportation of water masses was

23,3].

The prevailing wind direction is southwest, which, together with the bathymetry of the bed, is why there is not enough time for water to escape into the deeper areas in the center of the bay. As said in studies of Kheirabadi [4] and Ranjbar and Hajizadeh Zaker [5], GB is highly affected by three factors: a) the Caspian Sea, B) Wind forcing, and C) Geophysical factors in physical terms.

In figures 8 and 9, the background color shows the water level in GB. The water level fluctuates inside and outside of GB and in the eastern and western parts of the bay throughout the year. Its cause is the overflowing of rivers that mostly flow into it from the bay's east, southeast, and south sides. According to Figure (9), it is worth noting that the currents at the bay's entrance are much higher than in other parts of it. Also, from west to east, strong wind-induced currents are seen near the northern and southern coasts, and the average speed of the current on the northern and southern coasts is higher than in its interior areas. Even though the currents in the surface layer and bottom are similar for most of the year, we see a difference in the flow direction in the winter season.

The bay receives freshwater input from 10 small rivers and precipitation; discharge of all rivers into the bay is about 1.3 m³/s, and the precipitation rate is 30.7 cm/year for the bay. 62% of the freshwater inputs are from the Qareh Sou River, with a flow of 800 L/s. [1] With that said, rivers have not had a significant effect on the flow vectors, and the currents in winter and summer near the north and south coasts of the Bay cause slight changes in the water circulation pattern.

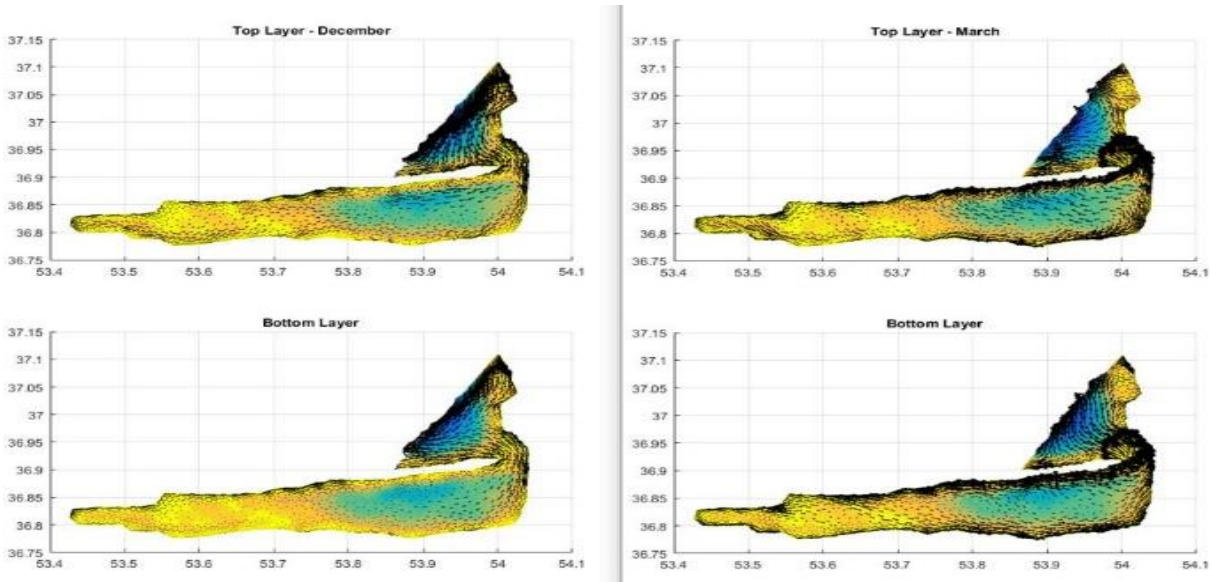


Figure 9. Currents vectors and depth in GB

The water level inside GB is influenced by several factors. One is the water level of the CS and the topography of the bottom of the GB. This study clearly shows that the water level inside GB also depends on the pressure parameter. The lack of pressure has affected the average velocity of currents.

The temperature inside the bay has changed sinusoidally in all places and all layers during different seasons, caused by the seasonal variability of atmospheric fluxes. This result directly correlates with the studies of Ranjbar and Hajizadeh Zaker [3]. The temperature on the northern coasts of the western side of GB experiences a temperature difference of 1 degree on average in all seasons of the year with other places in the west of the bay. Unlike the western part of the Bay, in the deep part of the Bay (middle), the distance between the temperatures in different layers is more different as we go deeper into GB's depth. The minimum temperature in the surface layer of water southeast of the bay occurs in profile 3, with a temperature of 2.4°C.

Temperature changes in the winter season are not more significant in any place inside GB than outside its mouth. The temperature in the coastal areas of GB is the highest, with 36.35°C in July and August. It reaches zero degrees in January on the southern coast, which is its lowest value. In former studies, the maximum temperature inside the bay was estimated at around 29-30°C. However, this paper indicates that the temperature inside the water body has accelerated over the past decade and shows a maximum degree of 36.57°C. This paper finds these effects directly putting GB under stress because of climate change..

Several suggestions are given below for future investigations on the restoration of GB:

1. The restoration of GB requires solutions compatible with the existing ecological and hydro morphological conditions and includes the scenario of long-term reduction of the Caspian Sea water level until the end of the 21st century.
2. According to the results of past studies in this regard and the topography and hydrography maps of the coast, finding the most suitable place to construct the canal can be very important.
3. The reduction of water self-purification in the GB due to the decrease in water volume and disconnection from the CS can also be investigated. Poor water quality has seriously affected the ecotourism and fishing industries on which people depend for their livelihood. As a result, building water quality models for the bay can help improve the residents' quality of life.
4. Predicting the effects of water level reduction on the degree of drought in the international wetlands of Gorgan, Gamishan and Miankaleh under the possible scenarios of water level reduction through computer simulation and using the output results of the model for appropriate planning for the development of vegetation in dry coastal areas to prevent dust. The region helps inland coastal communities such as birds to create ecological nests and increase the population.
5. Estimating the time required for the complete drying of GB and Miankaleh Wetland after being separated from the CS under a set of

climatic and hydrological factors governing the basin.

5. References

- [1] Ranjbar, M.H., Alaei, M.J. and Nazarali, M., 2019. A modeling study of the impact of increasing water exchange rate on water quality of a semi-enclosed bay. *Ecological Engineering*, 136, pp.177-184.
- [2] Bastami K, Bagheri H, Haghparast S, Soltani F, Hamzehpoor A, Bastami M (2012) Geochemical and geo-statistical assessment of selected heavy metals in the surface sediments of Gorgan Bay, Iran. *Mar Pollut Bull* 64:2877–2884
- [3] Ranjbar, M.H. and Hadjizadeh Zaker, N., 2018. Numerical modeling of general circulation, thermohaline structure, and residence time in Gorgan Bay, Iran. *Ocean Dynamics*, 68(1), pp.35-46.
- [4] Kosarev A (2005) Physico-geographical conditions of the Caspian Sea. In: *The handbook of environmental chemistry*. Springer
- [5] Kitazawa D, Yang J (2012) Numerical analysis of water circulation and thermohaline structures in the Caspian Sea. *J Mar Sci Technol* 17: 168–180.
- [6] Khairabadi, Hassan and Mohammad Wali Samani, Jamal and Nouri, Ruholah and Ranjbar, Hassan, 2014, 3D simulation of Gorgan Bay hydrodynamics by MIKE3 model FM 14th Iranian Hydraulics Conference, Zahedan, <https://civilica.com/doc/437909>
- [7] Qanqormeh Abdul Azim, Sharbaty Saeed, predicting the effect of the long-term trend of lowering the Caspian Sea water level on the life of Gorgan Bay.
- [8] Khairabadi, Hassan and Mohammad Wali Samani, Jamal and Nouri, Rooh Elah and Ranjbar, Hassan, 2014, 3D simulation of Gorgan Bay hydrodynamics by MIKE3 FM model, 14th Iranian Hydraulics Conference, Zahedan, <https://civilica.com/doc/437909>. Sharbaty, S. Hosseini, V. Taghizadeh, M.R. Imanpour and S. Gorgin, Two-dimensional modeling in Gorgan Bay Currents influence by sea level changes and wind pattern changes, Proceeding of first Conference of Caspian sea ecology, Sari, Iran, 2010. (In Persian)
- [9] Dr. Valizadeh, .(2019). Ph.D. Thesis, 3D Numerical Modeling of Circulation of Caspian Sea
- [10] khoshnavan, H. (2021). Caspian rapid Sea level fluctuation and intensity of displacement of the shorelines in the Gorgan Bay and Miankaleh coast', *International Journal of Coastal and Offshore Engineering*, 6(4), pp. 24-32.)
- [11] PourSufi, .(2015). Ministry of Jihad Agriculture Agricultural Research, Education and Promotion Organization. Iran Fisheries Science Research Institute - Inland Water Aquatic Reserve Research Center.
- [12] Ranjbar, H. (1392) 'Investigating the absorption capacity of Gorgan Bay in relation to the input of plant nutrients using numerical modeling, Master's Thesis, Graduate School of Environmental Studies, University of Tehran
- [13] DHI. (2007), User Manual Mike3 Flow Model FM, Hydrodynamic Module
- [14]. (Payandeh, A., Hadjizadeh Zaker, N., & Niksokhan, M. (2014). Numerical assessment of the nutrient assimilative capacity of Khur-e-Musa in the Persian Gulf. *Environmental Monitoring and Assessment*, 187, 1–14.)
- [15] (Ranjbar, M. H., & Hadjizadeh Zaker, N. (2014). Numerical simulation of currents in Gorgan Bay by PMO dynamics & MIKE 21 FM. Proceedings of 11th International Conference on Coasts, ports and Marine Structures (ICOPMAS), Iran, Tehran.)
- [16] *Marine Ecological Geography: Theory and Experience - Fashchuk, D.Y.* 9783642174445- Environmental Science and Engineering <https://books.google.com/books?id=B576PjBg0WYC>- 2011 Springer Berlin Heidelberg
- [17]. Sharbaty, Saeed. "Simulation of wind-driven waves in the Gorgan Bay." *Canadian Journal on Computing in Mathematics, Natural Sciences, Engineering and Medicine* 3.2 (2012): 40-44
- [18] Taheri, M., et al., 2012. Spatial distribution and biodiversity of macrofauna in the southeast of the Caspian Sea, Gorgan Bay in relation to environmental conditions. *Ocean Sci. J. Korean Ocean Research and Development Institute and The Korean society of Oceanography* 47 (2), 113–122. <https://doi.org/10.1007/s12601-012-0012-8>.
- [19] Cloern, J.E., and A.D. Jassby. 2008. Complex seasonal patterns of primary producers at the land-sea interface. *Ecology Letters* 11 (12): 1294–1303. <https://doi.org/10.1111/j.1461-0248.2008.01244.x>.
- [20] O'Boyle, S., R.Wilkes, G. McDermott, S. Ni Longphuir, and C. Murray. 2015. Factors affecting the accumulation of phytoplankton biomass in Irish estuaries and nearshore coastal waters: A conceptual model. *Estuarine, Coastal and Shelf Science* 155: 75–88. <https://doi.org/10.1016/j.ecss.2015.01.007>.
- [21] Darvishsefat, A., 2006. Atlas of protected areas of Iran. Assistance of ecology and biodiversity. Iranian Environmental Protection.
- [22] Kheirabadi, H., et al., 2018. A reduced-order model for the regeneration of surface currents in Gorgan Bay, Iran. *J. Hydroinform.* 20 (6), 1419–1435. <https://doi.org/10.2166/hydro.2018.149>.

- [23] Kouhanestani, Z.M., et al., 2018. Assessment of spatiotemporal phytoplankton composition in relation to environmental conditions of Gorgan Bay, Iran. *Estuaries Coasts*. Springer US 1–17. <https://doi.org/10.1007/s12237-018-0451-2>.
- [24] Sharbaty, S., 2012. 3-D simulation flow pattern in the Gorgan Bay in during summer. *International Journal of Engineering Research and Applications (IJERA)*, 2(3), pp.700-707.
- [26] Sharbaty, Saeed. (2012). Two Dimensional Simulation of Seasonal Flow Patterns in the Gorgan Bay. 2. 4382-4391.